AGU ADVANCING EARTH AND SPACE SCIENCE

Water Resources Research

RESEARCH ARTICLE
10.1029/2021WR030784

A Dynamic, Network Scale Sediment (Dis)Connectivity Model to Reconstruct Historical Sediment Transfer and River Reach Sediment Budgets

Marco Tangi[1], Simone Bizzi[2], Kirstie Fryirs[3], and Andrea Castelletti[1]

[1]Department of Electronics, Information, and Bioengineering, Politecnico di Milano, Milan, Italy, [2]Department of Geosciences, Università di Padova, Padua, Italy, [3]Department of Earth and Environmental Sciences, Macquarie University, North Ryde, NSW, Australia

Key Points:

- We present the new dynamic D-CASCADE model for network-scale river sediment (dis)connectivity modeling
- D-CASCADE successfully reproduced major historic geomorphological changes observed in the Bega river network after European settlement
- D-CASCADE is used to test future trajectories of basin-scale sediment transport and reach-scale sediment budget in the Bega river system

Supporting Information:

Supporting Information may be found in the online version of this article.

Correspondence to:

M. Tangi,
marco.tangi@polimi.it

Citation:

Tangi, M., Bizzi, S., Fryirs, K., & Castelletti, A. (2022). A dynamic, network scale sediment (dis)connectivity model to reconstruct historical sediment transfer and river reach sediment budgets. *Water Resources Research*, *58*, e2021WR030784. https://doi.org/10.1029/2021WR030784

Received 7 JUL 2021
Accepted 17 JAN 2022

Author Contributions:

Conceptualization: Marco Tangi, Simone Bizzi, Kirstie Fryirs, Andrea Castelletti
Data curation: Marco Tangi, Simone Bizzi, Kirstie Fryirs, Andrea Castelletti
Formal analysis: Marco Tangi, Simone Bizzi, Kirstie Fryirs
Funding acquisition: Andrea Castelletti
Investigation: Marco Tangi, Simone Bizzi, Kirstie Fryirs
Methodology: Marco Tangi, Simone Bizzi, Kirstie Fryirs, Andrea Castelletti
Project Administration: Andrea Castelletti

Abstract Modeling network-scale sediment (dis)connectivity and its response to anthropic pressures provides a baseline understanding of river processes and sediment dynamics that can be used to forecast future hydro-morphological changes in river basins. However, this requires a solid understanding of how a system is currently operating, and how it operated in the past. We present the basin-scale, dynamic sediment connectivity model D-CASCADE, which combines concepts of network modeling with empirical sediment transport formulas to quantify spatiotemporal sediment (dis)connectivity in river networks. D-CASCADE accounts for multiple factors affecting sediment transport, such as spatiotemporal variations in hydrological regime, different sediment grain sizes, sediment entrainment and deposition. Add-ons are included in D-CASCADE to model local changes in river geomorphology driven by sediment-induced variations in features such as channel width. We apply D-CASCADE to the well-documented Bega River catchment, NSW, Australia, where significant geomorphic changes to rivers have occurred post European colonization (after 1850s), including widespread channel erosion and sediment mobilization. The Bega catchment provides a useful case study to test D-CASCADE, as original source data on the historical sediment budget are available. By introducing historic drivers of change in the correct chronological sequence, the D-CASCADE model successfully reproduced the timing and magnitude of major phases of sediment transport and associated channel adjustments over the last two centuries. With this confidence, we then ran the model to test how well it performs at estimating future trajectories of basin-scale sediment transport and sediment budgets at the river reach scale.

1. Introduction

Sediment (dis)connectivity is a fundamental property of river networks, emerging from temporal and spatial interactions (or the lack thereof) among sediment of different composition and grain size, delivered to the river from sources with varying supply rates, timing, and spatial distribution. Hydro-morphological properties of river channels (e.g., width, gradient, and discharge) regulate sediment transport capacity and entrainment, transport, and deposition dynamics and rates. Spatiotemporal variability in the magnitude, frequency, and location of flood events that drive basin-scale patterns of discharge will also change the distribution and strength of these processes (Bracken et al., 2015; Fryirs, 2013; Fryirs et al., 2007; Heckmann et al., 2018; Sklar et al., 2017). To adequately and realistically model natural systems, these dynamics need to be properly accounted for in sediment transport models.

Direct or indirect anthropic alterations disrupt sediment (dis)connectivity, leading to major shifts in river channel morphology at both the local (e.g., reach) and network scales. As (dis)connectivity is a distributed property of river systems, multiple drivers, whose intensity and effects may be spatially and temporally heterogeneous, may produce positive or negative feedbacks that alter the operation of the sediment cascade (Bizzi et al., 2015; Fryirs, 2013; Gregory, 2019; Surian & Rinaldi, 2003; Vörösmarty et al., 2003; Wohl et al., 2019). Thus, the characterization of basin-scale sediment (dis)connectivity is critical for improving our capacity to quantify possible future alterations following anthropic disturbances, whether direct (e.g., construction and management of a reservoir, or removal of vegetation), or indirect (e.g., land use change, climate change, or implementation of restoration), and determine how to manage them (Kondolf, Gao, et al., 2014; Kondolf, Rubin, & Minear, 2014; Poeppl et al., 2020; Wohl et al., 2019).

Resources: Marco Tangi, Simone Bizzi, Kirstie Fryirs, Andrea Castelletti
Software: Marco Tangi, Simone Bizzi
Supervision: Simone Bizzi, Kirstie Fryirs, Andrea Castelletti
Validation: Marco Tangi, Simone Bizzi, Kirstie Fryirs
Visualization: Marco Tangi, Andrea Castelletti
Writing – original draft: Marco Tangi
Writing – review & editing: Marco Tangi, Simone Bizzi, Kirstie Fryirs, Andrea Castelletti

Traditional morphodynamic models allow for detailed modeling of river processes with high accuracy, but, due to high computational demand and in-situ data requirements, analysis is often limited to short and well-studied river reaches or segments, where the boundary conditions can be defined precisely (Briere et al., 2010; Lammers & Bledsoe, 2018). However, such models do not take into account the (dis)connected nature of sediment transport that occurs at the basin-scale (Merritt et al., 2003).

Recently, the increased availability of remotely sensed datasets has allowed characterization and interpretation of geomorphic processes at the scale of the entire river network (Bizzi et al., 2019; Demarchi et al., 2017; Schmitt et al., 2014). This has led to the development of novel numerical models of network-scale sediment (dis)connectivity (Czuba et al., 2017; Gilbert & Wilcox, 2020; Heckmann & Schwanghart, 2013; Schmitt et al., 2016a; Wild et al., 2021). These approaches aim to represent large-scale sediment transfer processes and therefore require empirical transport equations and pre-defined boundary conditions as inputs. This differs from more traditional models that use hydraulic and channel geometry interactions to simulate local-scale morphodynamic processes to derive transport rates. As a consequence, these new models trade off some accuracy so they can be run over longer timeframes and larger areas to produce results that characterize (dis)connectivity patterns among different components of the river network.

The CASCADE model (Schmitt et al., 2016a) is a network scale sediment connectivity model that describes the movement of material from many individual sources as separate transport processes called "cascades". Each cascade is identified by its provenance and carries a specific sediment volume that can be partly or completely deposited as it moves downstream, and interacts with other cascades. Thus, CASCADE can be used to quantify the rates at which each sediment source is connected with downstream reaches and to calculate the statistical properties of connectivity between different sediment sources and sinks.

Therefore, CASCADE can evaluate (dis)connectivity alterations due to changes in both sediment sources and network hydro-geomorphic features for any given type of disturbance event (whether natural or anthropic; Schmitt et al., 2018a, 2019). Tangi et al. (2019) expanded the description of the sediment cascade from a single grain size, to multiple grain size classes of varying volume or load. This advance allows for a more thorough representation of sediment supply and transport in a river network (Bizzi et al., 2021). CASCADE, however, is a static model that can only represent spatial (dis)connectivity at one point in time, under static network properties and features.

In this paper, we present D-CASCADE, a new dynamic, network-based sediment (dis)connectivity model that can be used to explore the spatiotemporal evolution of sediment supply and delivery across a basin. D-CASCADE maintains all the properties of the original CASCADE, but includes a temporal representation of sediment processes that is able to trace the position and movement of cascades over time, as well as across space. Thus, D-CASCADE can investigate the effects of multiple heterogeneous drivers of change that vary in magnitude, location, duration, or timing, as well as pinpoint and characterize the contribution of each driver to the cumulative change.

D-CASCADE is designed to be a flexible and highly customizable modelling environment that can be adapted for different purposes, data availability, and level of detail needed. The model allows for the inclusion of multiple modelling add-ons that are designed to simulate hydro-morphological processes that cannot be captured by the grid-based structure of D-CASCADE.

In this paper, we apply D-CASCADE to the Bega River network, NSW, Australia, with the objective of reproducing the known geomorphic changes and trajectories of river adjustment that have occurred due to anthropic disturbances post-European Settlement (ES). The Bega catchment case study was chosen to test D-CASCADE because of the wealth of well-documented and published data on river change and sediment budgets (e.g., see Brierley & Fryirs, 2013; Brooks & Brierley, 1997; Fryirs & Brierley, 2001; Fryirs et al., 2007). We return to the historical record and use the original source data to reconstruct the pre-ES river morphology. We then define the magnitude, timing, and location of dominant historic drivers of geomorphic change over the last 170+ years to set the boundary conditions for the simulation. Given the large uncertainties in the reconstruction of some historical parameters, a sensitivity analysis is used to explore different scenarios of geomorphic change in response to different hydraulic conditions over time. Knowledge of system evolution is then used to delineate possible trajectories of future geomorphological adjustments across the river network.

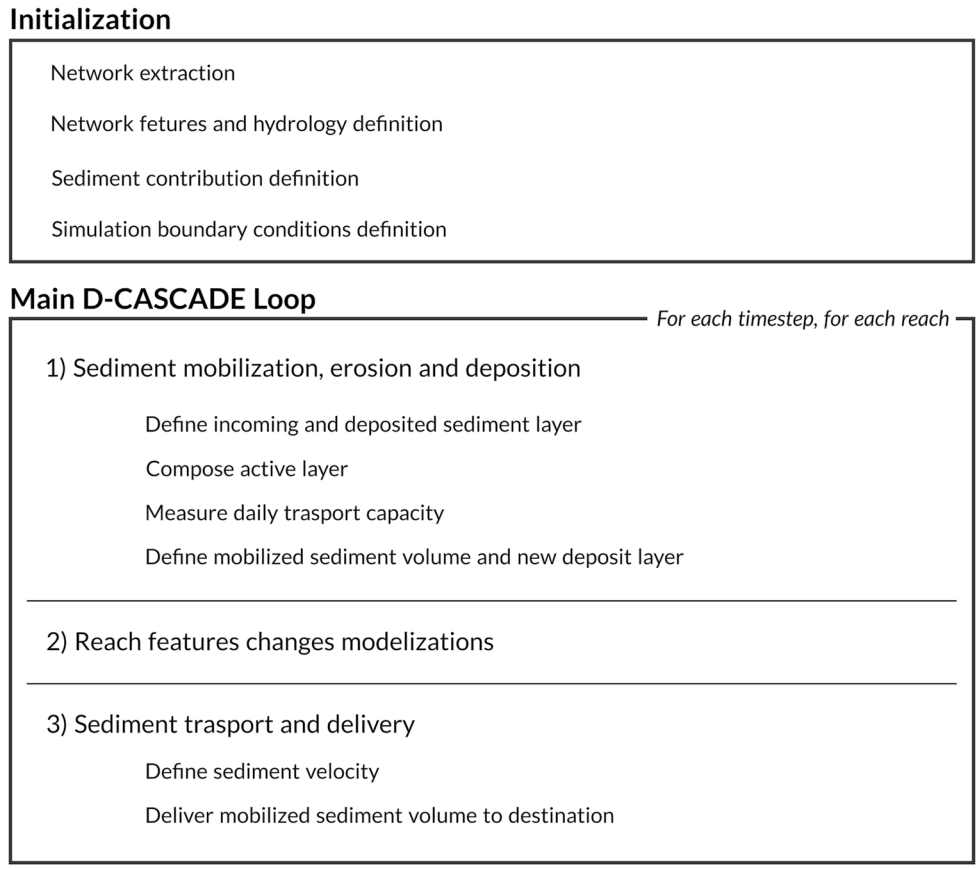

Figure 1. Modeling steps in the D-CASCADE framework.

2. Methodology

The structure, core components, and procedures of the D-CASCADE model are shown in Figure 1. The model setup is divided into two phases: initialization, and main D-CASCADE loop.

2.1. Initialization

The initialization phase defines the input data necessary to run D-CASCADE and delineates the structure of the simulation. The model's primary input is the river network, represented as a graph comprised of nodes and reaches, as per the static CASCADE model (Tangi et al., 2019). The reach is the core modeling unit in both versions of CASCADE and is defined as a section of the river network between two nodes characterized by homogeneous geomorphic and hydraulic features. Each reach is defined by a unique set of geomorphological features that use empirical formulas in the modeling framework to derive information on sediment transport (such as transport capacity and velocity) via empirical formulas. These features fall into three categories:

1. Static features, which are kept fixed for the entirety of the simulation and must be defined once for each reach.
2. Dynamic features, whose values may change in each timestep, and are defined a priori for each reach and for each timestep by the user.
3. Modeled features, whose changes are simulated in each timestep by a specific component in the modeling framework, and thus only require initialization for the first timestep.

The reach features used by D-CASCADE are reported in Table 1, together with their classification for the Bega case study. Depending on the confidence limits of knowledge of the study system and the data available, a feature may be better implemented as static, dynamic or modeled. For example, the active channel width may be kept constant (static), changed in each timestep by the user (dynamic) according to the discharge, or simulated by a

Table 1
Key Input Features, Possible Sources for Deriving Their Values, and How These Features are Reproduced in D-CASCADE

Features	Description	Classification for the Bega case study
Slope [m/m]	Channel slope. Derived from data surveys or Digital Elevation models (DEMs)	Static feature
Length [m]	Desired length of individual reaches. Depends on the partitioning method used on the network.	Static feature
Q [m^3/s]	Discharge in the timestep. Obtained from interpolation of gauging station datasets (Schmitt et al., 2016b) or spatially distributed hydrological models (Schmitt et al., 2018b).	Dynamic feature
Active channel width [m]	Width of the channel section in the timestep. Obtained from satellite imagery (Schmitt et al., 2014, 2016b, 2018b), field studies, or global data (Frasson et al., 2019; Yamazaki et al., 2014)	Modeled feature
Grain size distribution (GSD)	Grainsize distribution parameters of sediment in the river bed. Interpolated from available point sediment samples, expert-based assessments, or based on hypothesis regarding river sediment transport regimes.	Modeled feature
Manning's *n*	Manning's roughness coefficient for the bed material in the channel. Obtained from field data or estimated from the literature.	Dynamic feature
Sediment deposit [m^3]	Total amount of sediment stored in each reach, in each timestep. Estimated by field surveys, and expert assessments.	Modeled feature

specific component in the modeling framework to reproduce channel width changes due to sediment erosion (modeled), as in the case of the Bega case study. Moreover, the initialization phase also includes the definition of the boundary conditions of the simulation, such as its time horizon, the numerical precision in the measurement of the sediment volumes, and the provenance and quantity of sediment routed in the model.

Sediment volumes routed through the network may be derived from material initialized in the reaches as a sediment deposit, or as external, user-defined sediment contributions supplied to individual reaches in specific timesteps, for example, to reproduce sediment delivery from the hillslopes. Cascades are defined by the ID of the reach where the volume was initially delivered or stored, and the total sediment volume transported [m^3], subdivided into different grain size classes. The size and composition of the sediment classes are pre-determined and defined in the initialization phase, and are selected according to the composition of the material transported and the level of detail desired.

2.2. Main D-CASCADE Loop

The main D-CASCADE loop, which constitutes the core of the modeling framework, is comprised of a series of operations, broadly described in Figure 1, which are repeated for each reach and for each timestep as: (a) mobilized sediment definition, (b) change in geomorphic features, (c) and sediment delivery.

2.2.1. Mobilized Sediment Definition

In each reach, the total volume mobilized and transported downstream in each timestep is comprised of cascades either delivered from upstream in the previous timestep, stored in the deposit layer or both.

The deposit layer is conceptualized as a series of distinct tiers stacked on top of each other, with each tier comprised of a single cascade (Figures 2a and 2b). This modeling structure guarantees that newly deposited cascades form a tier above the previously deposited material, and at the same time entrained sediment is removed from the upper tiers of the deposit first. At any timestep t, the total sediment volume [m^3] in the deposit and the incoming cascades layers of a reach is measured as:

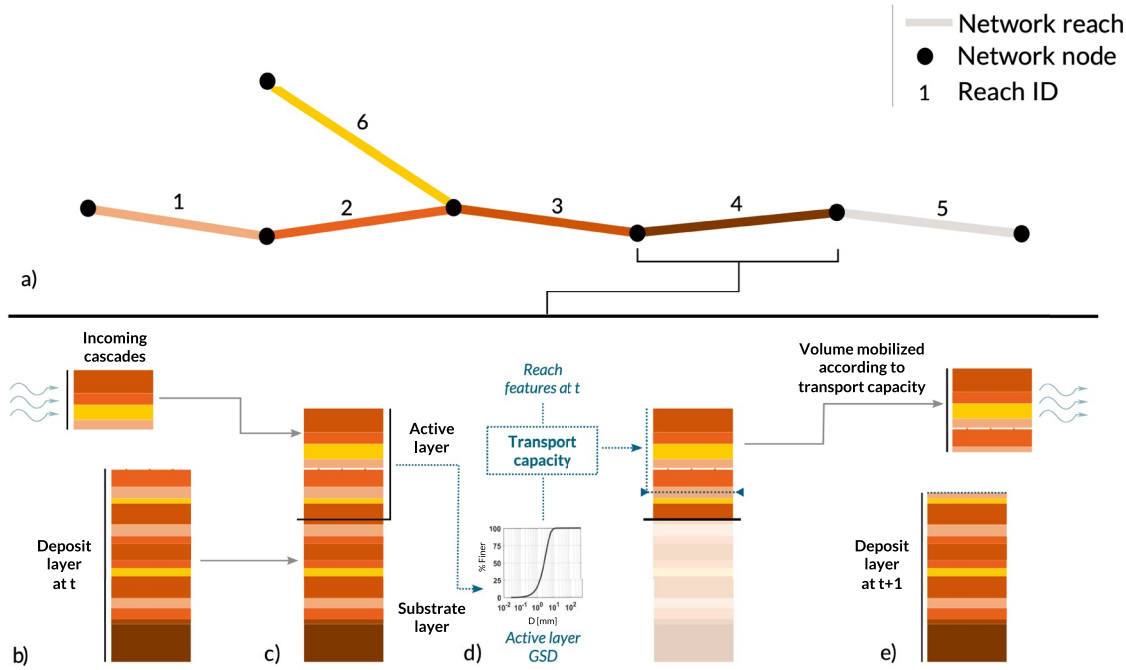

Figure 2. An example of how the mobilized sediment volume is defined in a reach in a single model timestep. (a) shows the modeled network as a graph comprised of reaches and nodes, (b) to (e) show the passages to define the mobilized sediment volume for reach 4. The colors of the tiers indicate the reach of provenance in the network. In (b) the model extracts the incoming cascades and deposit layer in the timestep, in (c) the deposit is divided into active and substrate layer, in (d) the model calculates the transport capacity for the sediment in the active layer, according to the layer Grain Size Distribution (GSD). Finally, in (e) the mobilized volume and new deposit layer are defined.

$$V_d(t) = \sum_{\substack{\text{all cascades } c \\ \text{in the deposit} \\ \text{layer } d \text{ at time } t}} V_d(c,t) \tag{1}$$

$$V_i(t) = \sum_{\substack{\text{all cascades } c \\ \text{in the incoming} \\ \text{layer } i \text{ at time } t}} V_i(c,t) \tag{2}$$

where $V_d(c,t)$ and $V_i(c,t)$ are the total volumes transported by individual cascades located respectively in the deposit and incoming layers at time t, given by the sum of sediment volumes for each sediment class.

As illustrated in Figure 2c, the incoming sediment cascades are stacked above the deposit layer to form a single column, with volume $V_{\text{tot}}(t) = V_d(t) + V_i(t)$. This volume is then divided into an active layer $V_a(t)$ and a storage/subsurface layer, according to the maximum active layer volume $V_a^{\max}(t)$ (similar to the procedure used in Czuba, 2018 and Czuba et al., 2017), measured as:

$$V_a^{\max}(\text{t}) = W(t) d_a l \tag{3}$$

where l is the reach length [m], $W(t)$ [m] i s the channel width at time t. d_a [m] is the active layer thickness, which indicates the depth of the sediment layer that can be mobilized in a single daily timestep, defined either as a constant or as a variable in space and time according to the hydraulic and geomorphic conditions of the reaches. Cascades in the top part of the column are put in the active layer until its volume $V_a(t)$ reaches the maximum volume $V_a^{\max}(t)$ or there are no more cascades available. If a cascade is situated on the boundary between active and substrate layers, it is divided according to the remaining available volume in the active layer.

The volume $V_m(t)$ mobilized in the reach at time t is determined by the sediment transport capacity, that is, the maximum sediment discharge passing through a section allowed by the hydro-morphological characteristics of the reach in the timestep considered. The instantaneous transport capacity Q_s [m^3/s] can be calculated using empirical formulas, which requires a definition of the grain size distribution (GSD) or the median grain size (D50; Jr & Yang, 1989). The GSD used in the sediment transport is relative to the sediment volume in the active layer (Figure 2d). The instantaneous transport capacity is then converted into daily transport capacity to determine the mobilized volume $V_m(t)$ for timestep t. Thus, the cascades in the active layer are mobilized starting from the top layer, until a volume equal to the $V_m(t)$ is reached or the active layer is emptied. These cascades will be transported downstream. Conversely, the volume not mobilized in the active layer is stacked on top of the storage layer to form the new deposit layer (Figure 2e).

D-CASCADE, like its predecessor, can support a wide range of transport capacity equations, so that the model can be adapted to simulate the hydro-morphological characteristic of the case study under consideration.

2.2.2. Change in Geomorphic Features

Selected modeling add-ons can be used to quantify changes in modeled geomorphic features between timesteps from the variation of sediment storage defined in the previous step. These add-ons can include traditional 2D or 3D morphodynamical modeling techniques, or a simplified model calibrated on observed historic channel evolution. For the Bega case study we included two components to update the active channel width and to account for overbank flooding. (See Add-ons modeling components section and Text S2 in Supporting Information S1).

2.2.3. Sediment Delivery

The mobilized volume in each reach is delivered downstream according to the characteristic velocity of sediment $v_s(i)$ of each reach i. The rate of transport of a mobilized sediment volume in the $i-th$ reach is defined as:

$$v_s(i) = \frac{Q_s(i)}{W(i)\ H_a} \tag{4}$$

where $Q_s(i)$ is the instantaneous transport capacity of the mobilized sediment in reach i [m^3/s], $W(i)$ is the channel width [m] and H_a is the characteristic vertical length scale for sediment transport [m], which can be a function of the water height or kept constant. In reality, the characteristic velocity varies substantially depending on a variety of factors including the composition of the solid material transported and the hydro-morphological conditions of the river reach. This formulation has been used in other distributed sediment models (Czuba & Foufoula-Georgiou, 2014; Hassan et al., 1991) and guarantees an estimate of sediment velocity that is useful for large-scale modeling efforts. However, Equation 4 provides a single estimation of sediment velocity for the mobilized sediment volume, without discriminating between different sediment classes. For each sediment volume $V_m(t)$, the model first derives sediment velocity for all the downstream reaches, from which it obtains the daily traveling distance, and then the destination reach, where the material will be delivered in the next timestep from the incoming layer $V_i(t+1)$. Sediment leaving the network through the outlet is stored in an appropriate, out-of-bounds layer.

3. Application to the Bega River Basin

Using the D-CASCADE modeling framework, we aim to test whether the most impactful geomorphic changes observed in the Bega River basin post European settlement (i.e., erosion and sediment release from valley fill swamps, channel expansion along the lowland plain, and sediment slug formation and movement), as well as recreate and model the sediment budget.

For the model parameterization, we first define the network features and the historic hydrology. We then introduce the modeling components for the geomorphic changes and the simulation structure. Finally, we define validation parameters for the model outputs based on literature and available data.

10.1029/2021WR030784

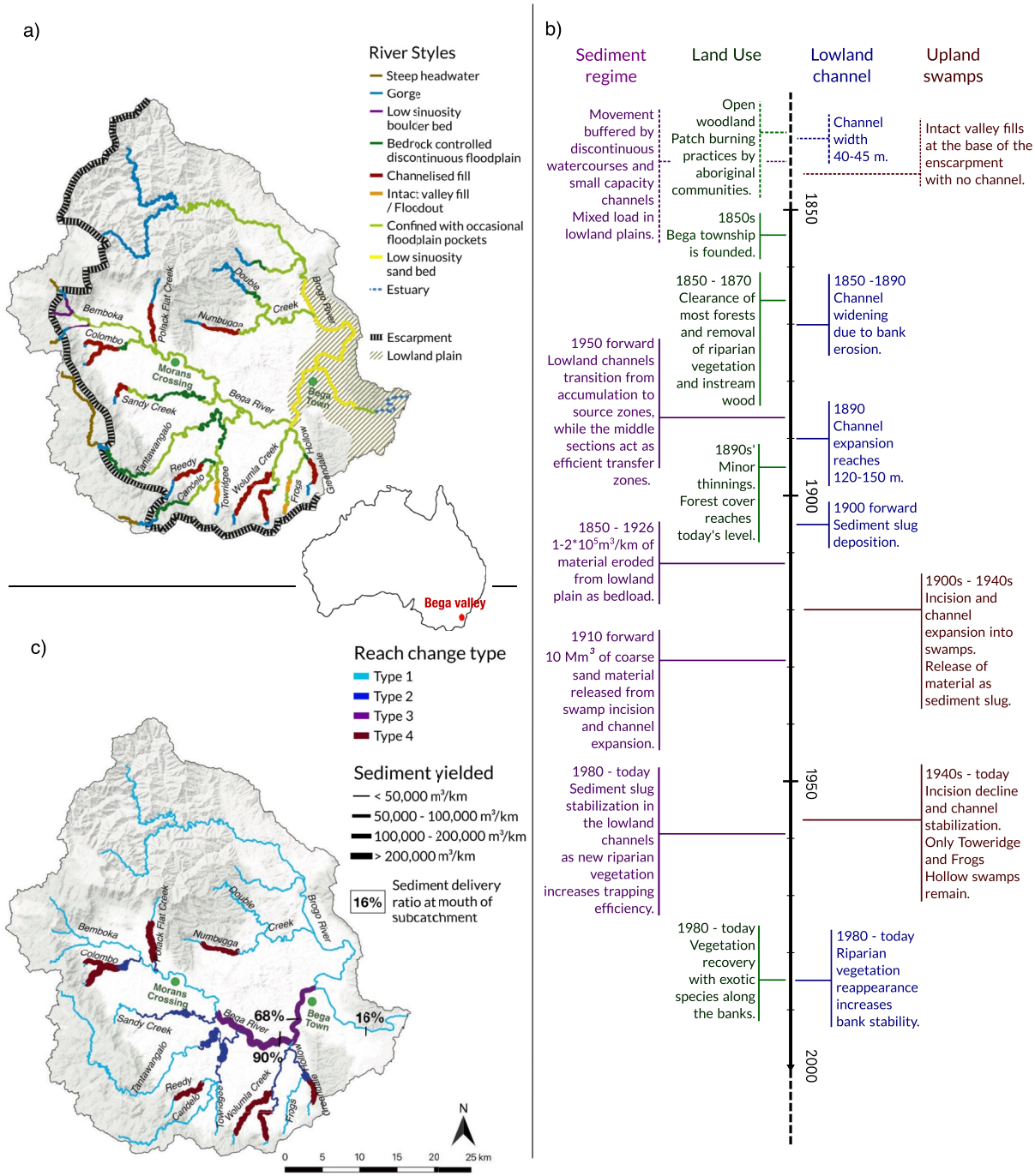

Figure 3. Features and timeline of changes in the Bega River valley. (a) Present-day River Styles in the Bega catchment, NSW, Australia; defined by Brierley and Fryirs (2000). Channelized fills were originally intact valley fills or swamps, but due to anthropic interference have experienced widespread erosion, incision and sediment release. (b) Timeline of the major geomorphological changes in the Bega catchment from 1850 to 2020. (c) Classification and sediment yielded since European settlement for the reaches of the Bega River network (in m^3/km) as defined by Fryirs and Brierley (2001). The amount of sediment yielded is represented by the line thickness. Sediment delivery ratios used for validation of the model outputs are also displayed.

3.1. Bega River Case Study

The Bega River basin is located on the south coast of NSW, Australia, and drains an amphitheater-shaped area of 1,930 km^2 (Figure 3a). An escarpment encircles the catchment, rising to 1,200 m asl. The catchment topography is dominated by rounded hills and confined and partly confined rivers. A short, alluvial lowland plain occurs

downstream of the Wolumla Creek confluence and extends to a choke-point gorge near the coast. The climate is characterized as temperate, but there can be prolonged periods of drought and no-flow that are abruptly broken by intense rain events that produce floods. The largest flood on record, in February 1971, had a discharge of 1,800 m^3/s at Morans Crossing (Figure 3a). A technical report by Cardno (2018) estimated that a flood event with 1% of annual exceeding probability, similar to the 1971 flood, could have a discharge of 10,400 m^3/s near the outlet.

The dramatic landuse and geomorphological changes to rivers that occurred following European colonization in the 19th century have been well-documented in the literature and are summarized in Figure 3b (Brierley et al., 1999; Brierley & Fryirs, 1998, 2000; Brooks & Brierley, 1997; Fryirs & Brierley, 1998, 1999, 2001, 2005; Fryirs et al., 2018). These changes resulted in a complete alteration of the sediment budget and regime for the system (Figure 3b). The post-ES sediment budget for the Bega catchment was published in Fryirs and Brierley (2001) (see Figure 3c).

3.2. Network Features Definition

River networks of the Bega basin were extracted using a Digital Elevation Model (DEM) provided by Geoscience Australia, with 2 m resolution, using the Topotoolbox software (Schwanghart & Scherler, 2014). Uniform reaches with an average length of 2 km were extracted, excluding reaches corresponding to former valley fills (swamps). Reaches corresponding to former valley fills are considered sediment sources and therefore extracted as a single channel without segmentation, to avoid sediment stagnation between consecutive source reaches. In total, the network is partitioned into 263 reaches.

To model the historic geomorphological changes in D-CASCADE, reaches are classified into 4 categories according to the type and magnitude of geomorphic changes experienced (Figure 3c):

1. Type 1 reaches are located above the escarpment line or along still vegetated river stretches that experienced no significant morphological changes.
2. Type 2 reaches are in the middle parts of the basin and have experienced minor channel expansion.
3. Type 3 reaches are in the lower part of the basin and have experienced substantial channel expansion.
4. Type 4 reaches are the valley fill reaches at the base of the escarpment that were affected by incision into swamps.

Modern day values of channel width, bed grain size distribution, and channel roughness coefficient are obtained from satellite images and field surveys, and historical data is drawn from the published literature. Elevation data from the DEM are used to derive channel slope; as no data on pre-ES channel gradient are known, we assumed slope to be a static network feature.

For type 2 reaches, the pre-ES channel width is set equal to 80% of the current value, to account for a 20% expansion in width. For type 3 reaches, the channel width is expanded from 40 to 135 m before 1890, while the original bed grain size is assumed equal to the estimated pre-ES bedload (Brooks & Brierley, 1997). For type 4 reaches, the last remaining intact swamps in the network are used as pre-ES analogs. These swamps are relatively wide (150–180 m) and steep (0.02–0.028). The types of sediment released from type 4 reaches is medium to coarse sand (1–1.4 mm) as documented in Fryirs and Brierley (1998) for the valley fill stratigraphy. Due to the lack of historical datasets, grain size distribution for type 1 and 2 reaches are assumed equal to present day value.

To derive values of flow stage height and velocity, the model uses the Manning-Strickler formula (Manning et al., 1890), which requires information for the roughness of the reach using the Manning's roughness coefficient. For the pre-ES condition, we assigned a relatively high roughness coefficient for all reaches, given the known presence of dense riparian vegetation and wood in the channels, equal to 0.2 for type 4 reaches and 0.1 otherwise. Roughness coefficients associated with vegetative recovery after 1980 have been defined using expert judgment as well as historic and contemporary satellite images. For example, in the lowland channels, roughness shifts from 0.1 pre-ES, to 0.04 after riparian vegetation removal, to 0.08 today with vegetative recovery.

By 2001, around 90% of the mobilized volumes were delivered to the lowland plain channels. Only around 16% of the released material has been delivered to the estuary (Fryirs & Brierley, 2001; Figure 3c). These volumes are used in the simulation to initialize the pre-ES sediment deposit in each reach, assuming uniform grain size

distribution. Distributed sediment input from the hillslopes are not considered, as hillslope sediment supply is decoupled from valley bottoms in this system, as in other equivalent systems in southeastern Australia (Brooks & Brierley, 1997; Wasson, 1994; Wasson et al., 1996).

3.3. Reconstruction of Hydrology

As D-CASCADE models a daily timestep, a complete simulation of the full time horizon would require continuous daily discharge data for all 263 reaches over 170+ years, which are not available. Therefore, given that most of the sediment movement along the Bega River network occurs during intermittent flood events, we have only simulated the daily timesteps when historic flood events with a 1-year relative flood return period (RP) or greater occurred, and assumed sediment transport to be nil or negligible otherwise. For detailed information on the reconstruction of hydrology, refer to Supporting Information S1.

In total, 168 daily flood events have been identified. Historical hydrological datasets from 1850 are only available for gauge height and relative flood RP in specific locations. To account for uncertainty in the correlation between gauge height, flood RP, and discharge, we defined four scenarios that are designed to cover a wide range of possible discharge conditions. Each scenario classifies each flood event, extracted from the historical stage height at recorded at a specific gauge station (Morans Crossing), into a RP class (1-, 2-, 5-, 10-, 20-, 50-, 100-year flows). The discharge for each reach is then correlated to each flood class as determined by the Australian Rainfall and Runoff (ARR) hydrological model (Fryirs & Brierley, 2001; Pilgrim et al., 1987). The scenarios are: Medium discharge scenario (MedQ), High discharge scenario (HighQ), Low discharge scenario (LowQ), and Mixed discharge scenario (MixQ). The MixQ scenario is designed to account for higher flood magnitude in upstream reaches compared to lowland reaches, and then to increase sediment erosion and release in the type 4 reaches. With the MixQ scenario, the same flood event is classified in a higher PR class in type 4 reaches, and in a lower class otherwise.

To explore future sediment transport trajectories in the network, we created 100 scenarios lasting 100 years each, assuming a maximum of one flood event per year, by generating independent flood events extracted from the yearly probability distribution of the historical data set.

3.4. Add-Ons Modeling Components

For the Bega case study, we introduce two add-ons to D-CASCADE to reproduce changes in channel width and the effect of overbank floods on the in-channel sediment storage. These components are described in detail in Text S2 in Supporting Information S1.

The channel expansion add-on simulates channel expansion caused by bank erosion and associated change in channel width by increasing the width value proportionally to the erosion of the initialized reach sediment budget, up to present-day conditions. This component is based on a simplified correlation extracted from reconstructions of historical channel evolution for the lowland reach. By doing this, the add-on links historical channel expansion with the removal of the initial sediment budget, meaning the model assumes any mobilization of the original sediment store in the reaches directly and immediately affects channel width. Despite the two processes not always being correlated, in the Bega River this hypothesis is supported by field evidences and historical reconstructions. For the lowland type 3 reaches, Brierley et al. (1999) reported that the initial channel expansion from 40 to 135 m was not accompanied by bed incision, and the channel expansion occurred into channel bank (floodplain) materials. For the type 4 valley fill reaches, Fryirs and Brierley (1999) reported that incision during phase 2 was closely followed by channel expansion of up to 20–50 m due to mass failure and bank toe erosion. As the initialized sediment deposit can only decrease as material gets eroded, modeled channel expansion is irreversible.

The overbank flooding component accounts for a portion of the discharge going overbank during particularly large floods, which decreases the potential for sediment erosion on the channel bed. This is especially important in the lowland reaches of the Bega system, where overbank flooding has historically led to sediment deposition on the floodplains and lower erosion potential of the channel bed. In each timestep, this add-on reduces the value of the discharge used to quantify the erosion of the deposit layer to a value corresponding to the highest non-overbank flood, while sediment transport and velocity remain unaltered.

Table 2
Timeline of Morphological Drivers Introduction and Add-Ons Activation in the Historic Simulations for Each Reach Types and Temporal Phases

	Phase 1 (1850–1900)	Phase 2 (1901–1910)	Phase 3 (1911–1980)	Phase 4 (1981–2020)
Type 1	• Channel roughness decreased linearly to pre-vegetative recovery values	• Overbank flood add-on component is active	• Overbank flood add-on component is active	• Channel roughness increased linearly to present day values where vegetative recovery is observed • Overbank flood add-ons component is active
Type 2–3	• Channel roughness decreased linearly to pre-vegetative recovery values • Sediment deposit made available for erosion proportionally to the changes in channel roughness • Channel width increased up to present day value as modeled by the channel expansion add-on	• Overbank flood add-on component is active	• Overbank flood add-on component is active	• Channel roughness increased linearly to present day values where vegetative recovery is observed • Overbank flood add-ons component is active
Type 4	No changes	• Channel roughness decreased linearly to pre- vegetative recovery values • Channel width decreased linearly to 10 m	• Channel width increased up to 50 m as modeled by the channel expansion add-on	Channel roughness increased linearly to present day values where vegetative recovery is observed

3.5. Simulation Structure

We introduced the drivers of geomorphological change in the modeling environment in a temporal sequence relative to known phases of historical channel change. Table 2 describes the structure and length of each phase and summarizes how and when the different drivers of change are introduced to the simulation. The temporal phases are:

1. Phase 1 (1850–1900): vegetation removal along lowland reaches that resulted in bank instability and channel expansion.
2. Phase 2 (1900–1910): valley fill incision and channel expansion along type 4 reaches.
3. Phase 3 (1911–1980): delivery and stalling of the sediment slug along the lowland plain channel and floodplain.
4. Phase 4 (1981–2020): vegetation recovery and subsequent decrease in sediment mobilization.

In this study, we consider seven sediment classes from very fine sand to pebbles (−5.5, −4, −2.5, −1, 0.5, 2 and 3.5 φ in Krumbein logarithmic scale, corresponding to 45, 16, 5.6, 2, 0.70, 0.25, 0.088 mm). The active layer thickness d_a (see Equation 3) and the vertical length for sediment transport H_a (see Equation 4) are kept constant in all reaches and equal to 1 and 0.1 m respectively (Czuba, 2018), and the sediment porosity $\phi = 0.4$ (Wu & Wang, 2006). To avoid excessive computing time and data storage, new sediment cascades are defined only if they carry at least 0.1 m^3 of sediment in at least one grain size class.

The transport capacity is calculated using the Ackers-White formula (Ackers & White, 1973), the bedload transport capacity formula also employed in Fryirs and Brierley (2001) as a best fit for sand and fine gravel bed rivers like the Bega. The formula requires estimation of D_{35}, obtained via interpolation of the grain size distribution of the active layer. Ackers-White is a total transport capacity formula, so the Molinas and Wu partitioning formula (Molinas & Wu, 2000) is used to derive fractional transport capacity for each sediment class.

3.6. Validation Parameters

To quantify how the D-CASCADE model simulation performs at reproducing quantifiable effects of major historical changes observed in the network, we defined four indicators based on field data and historical reconstruction, which compare the model outputs for the 2000s with field data collected in the same years (Brooks & Brierley, 1997; Fryirs & Brierley, 2001):

1. SedDelRt: Fryirs and Brierley (2001) extrapolated from field data the sediment delivery ratio (labeled SedDelRt) of the mobilized deposit at the mouth of different subcatchments since post-ES. We can derive sediment delivery ratio (SDR) from the model outputs by comparing the amount of sediment, deposited or mobilized, present in a subcatchment at time t with the same value at $t = 1$

$$\mathrm{SDR}(i,t) = \sum_{j=ur\_i}(V_d(j,t) + V_m(j,t)) \Big/ \sum_{j=ur\_i}(V_d(j,1) + V_m(j,1)) \quad (5)$$

where $\mathrm{SDR}(i,t)$ is the sediment delivery ratio in reach i at time t and ur_i is the set of all reaches situated upstream reach i, i included. In particular, we used the sediment delivery ratio in 3 different downstream locations as indicators (see Figure 3c): at the Bega River just before the Wolumla Creek confluence (SDR = 90%), the Bega River at Bega township (SDR = 68%), and just before the estuary (SDR = 16%). The sharp decrease in SDR between these sections is indicative of one of the major morphological changes observed, that is, the formation and trapping of a sediment slug in the lowland sections of the river.

2. Type 4 - % incised: According to Fryirs and Brierley (2001), sediment material initialized in the deposit layer of type 4 reaches (Figure 3c) should have been completely transported downstream by 2001. By measuring the percentage of total sediment initialized along these reaches eroded by 2001, we can validate if the methodology used to model sediment erosion is sufficient to reproduce incision of the valley fills and subsequent channel expansion.
3. Type 3 – Width: Validates whether the channel expansion add-on is able to reconstruct the historic changes in channel width along the lowland plain (Brooks & Brierley, 1997) by comparing the modeled average channel width with present day field-measured values.
4. Type 3 – D50: Check whether the model is able to replicate the coarsening of bed material grain size in the lowland reaches, and therefore the change in sediment regime from mixed load to bedload, by determining whether the average D50 of the modeled bed material matches the field-measured present day average of 1.4 mm (Brooks & Brierley, 1997).

4. Results

4.1. Historical Sediment Transport Trajectories

Figure 4 shows the D-CASCADE simulation outputs for the MedQ scenario, for selected sections of the river network. To aid in data visualization, lowland reaches are grouped into 4 different sections (Figure 4a, from A to D), each of which is comprised of 3–9 reaches. Total sediment volume in each timestep is defined as the sum of the mobilized volume $V_m(t)$ and the deposit layer $V_d(t)$ of all reaches in a section. Figure 4b shows the evolution of total sediment volume, normalized by section length, and channel width for the lowland sections in the simulation horizon. D-CASCADE provenance tracing allows us to categorize the total volume according to the original supply location. In this case, we distinguish between provenance from type 2 and 3 or type 4 reaches.

According to the model, channel expansion in type 2 and 3 reaches occurred between 1850 and 1900, mostly driven by large flood events, following a pattern similar to the historic trajectories (black dots in Figure 4a). Before 1900, all the bank material that was available has been eroded and channel width increases to present-day values. Most bank material (green in Figure 4b) is transported downstream, depositing predominantly in section C. After 1900, sediment released from incision of the valley fills (red in Figure 4b) transits easily through section A, before accumulating mostly in sections B and C.

Figure 4c shows trajectories for type 4 reaches for the MedQ scenario. Before 1900, all simulations show that sediment release from type 4 reaches is almost non-existent due to the unincised nature of the valley fills, characterized by no channel and high surface roughness that greatly reduces transport capacity. After 1910, swamp drainage and channelization lead to channel incision and sediment slug formation, which continues for the rest of the simulation horizon. Variations in the hydrology of each reach explains the wide range in sediment depletion trajectories, for example, Reedy and Colombo Creeks are mostly emptied before 1950, while Pollacks Flats, Greendale and South Wolumla Creek retain material past the year 2000.

After 1980, an increase in riparian vegetation and channel roughness leads to a visible decline in sediment mobilization in both upstream and downstream reaches, even during large floods.

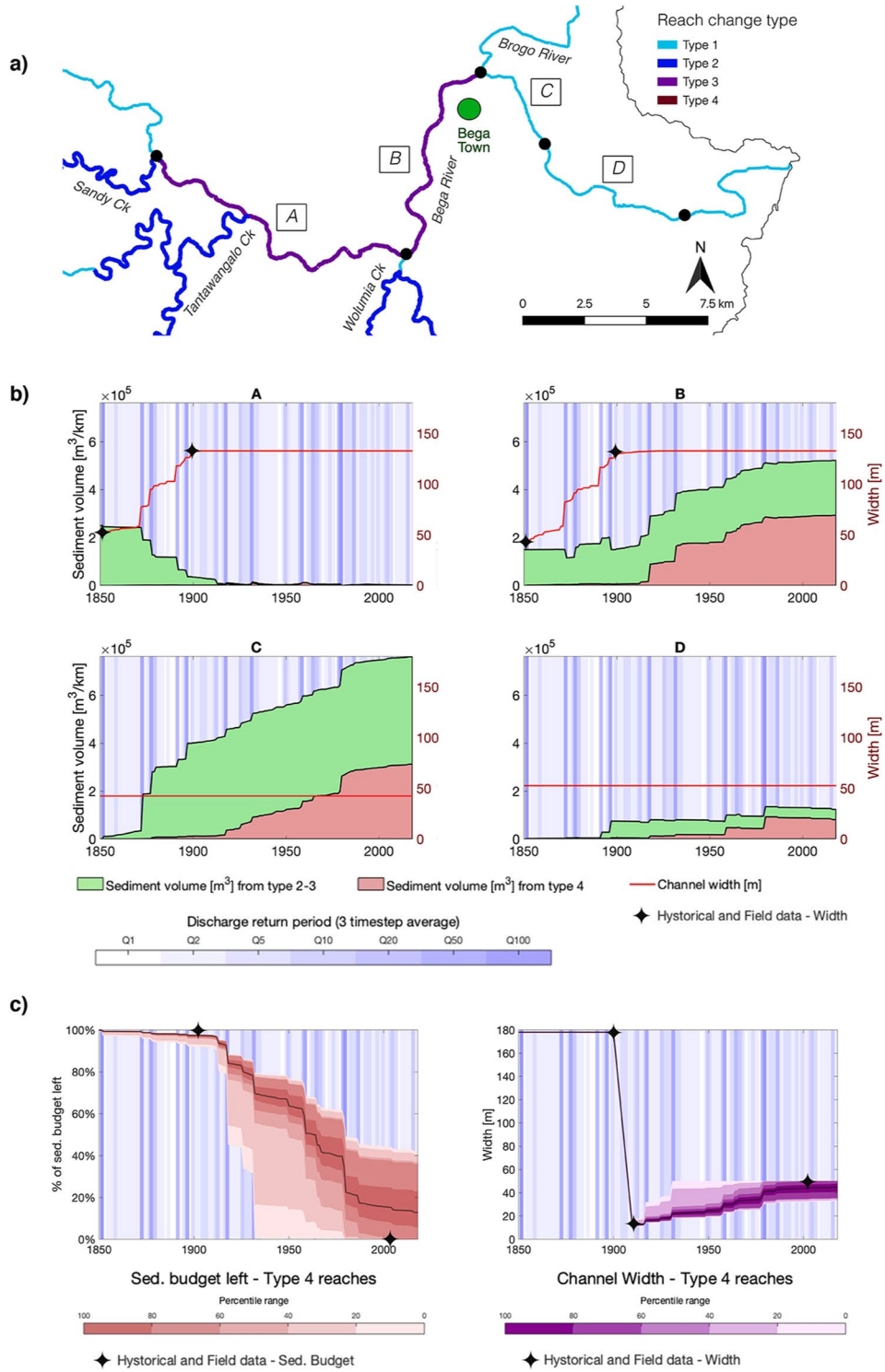

Figure 4. Variations in total sediment volume (normalized by section length) and network features in different locations in the river network for the MedQ scenario. The 4 downstream sections are identified in figure (a). Bars on the background of (b) and (c) indicate the flood RP each year, with a 3 timestep average. Black diamonds indicate data from hystorical reports in the year they are collected. Panel (b) show trajectories for the downstream reaches, separating sediment from channel expansion (type 2 and 3, in green) from material from incision of valley fills (type 4, in orange). The figure also shows channel expansion due to bank erosion (red lines). Panel (c) shows the decrease in percentage of the original sediment budget in type 4 reaches, following swamp drainage, incision, as well as channel expansion. A Montecarlo fan chart is used to visualize the combined range of values for type 4 reaches. Each color gradient defines a 20% frequency range of trajectories.

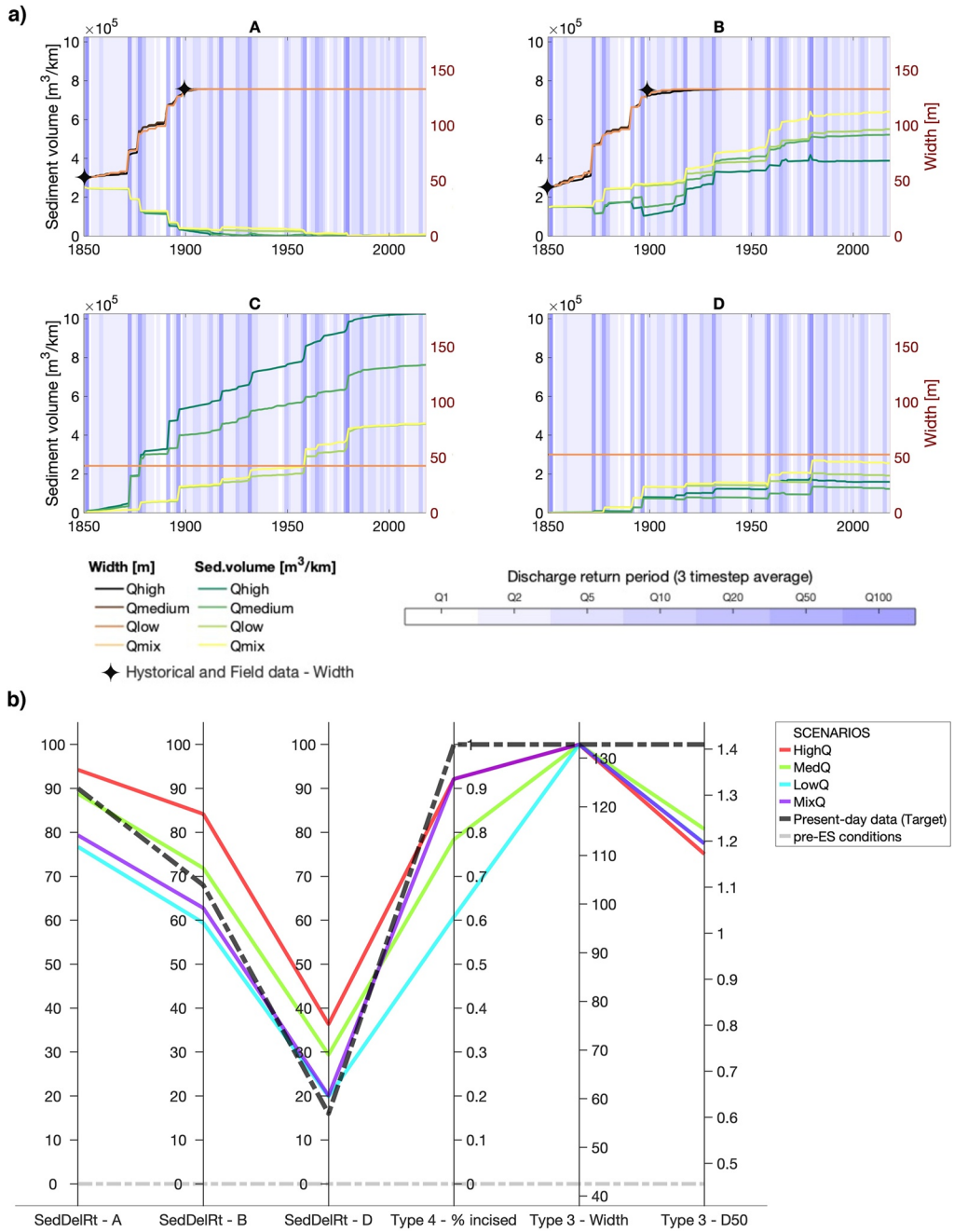

Figure 5. D-CASCADE model output and performances for the different hydrology scenarios. (a) Variation of total sediment volume and channel width along the lowland plain, for the four hydrological scenarios. Discharge is shown for the HighQ scenario. (b) Performance of the four hydrological scenarios for the six validation parameters. The gray and black dotted lines represent, respectively, the pre-ES and the present-day values for the parameters. MixQ scenario indicators (purple line) overall appear more similar to the target values (black line).

Figure 5a shows sediment delivery and deposition in the lowland reaches for the four hydrological scenarios. Most noticeably, under the HighQ and MedQ scenario, less sediment is stored in section B, and more in section C downstream of the Brogo confluence. Channel expansion rates remain largely the same across all scenarios.

The performance of the four scenarios for the four validation parameters are shown in Figure 5b. Sediment delivery of the material initialized follows similar patterns, as all scenarios present sediment sinks along the lowland

plain (Section B-C) while sections A and to a lesser extent D function as sediment source and transfer zones. Consequently, all scenarios show a clear decrease in sediment delivery between sections B and C.

Conversely, lowland channel expansion in all scenarios follows very similar trajectories, reproducing the pattern defined by historical observations (black dots in Figure 5a), with channel width reaching present-day conditions around 1890–1900. All simulations reproduce the coarsening of bed material along the lowland plain (Type 3 - D50 indicator).

Scenarios with the highest discharge in type 4 reaches (HighQ and MixQ) exhibit more pronounced erosion of valley fill sediment (Type 4 – % incised indicator), while LowQ and MedQ are associated with lower percentages in both parameters.

Overall, the MixQ scenario seems to perform the best for the validation criteria defined. This was expected, as MixQ has the multiple advantage of ensuring frequent high discharge on type 4 reaches that guarantees a high incision rate (Type 4 -% incised indicator) and sediment supply upstream (SedDelRt-A indicator), while also reducing flood event intensity in the lowlands to produce lower rates of sediment mobilization and a low sediment delivery ratio to the outlet (SedDelRt-D indicator).

4.2. Forecasting Future Sediment Transport Trajectories

As the MixQ scenario performed the best relative to the majority of the validation criteria, we used this classification method to generate discharge values for 100 future discharge scenarios with which to run forecasting exercises.

The red lines in Figure 6a show the projected range of variation of sediment volume and sediment delivery ratio for the downstream sections as defined in Figure 4a. This simulation runs for 100 years from 2020 to 2120. Type 4 reaches provide little further insight on system evolution because they are largely already depleted of sediment. For the lowland plain reaches, instead, it is forecast that the trend of sediment delivery from upstream will persist into the future, as any remaining material from upstream is delivered. However, a noticeable increase in sediment delivery only occurs in section B. Over the next 100 years a slow increase in sediment delivery ratio is forecast (brown lines in Figure 6b). This trend is more pronounced in upstream sections, as sediment from upstream is delivered to section B. While the majority of sediment remains trapped in section C, a small fraction does exit the system, as shown by the very small increase in sediment delivery ratio to the outlet and the decrease in volume in section D.

The simulated stagnation of the sediment slug is most likely a consequence of the high channel roughness associated with vegetative recovery (Fryirs et al., 2018). To check whether removal of riparian vegetation in the future would affect sediment transport, we ran the same future discharge scenarios, but with channel roughness across the whole river network set to pre-vegetative recovery values (blue lines in Figure 6a). The results show an increase in mobility in this scenario, and a subsequent increase in sediment delivery ratio along the lowland reaches and to the basin outlet (blue lines in Figure 6b).

5. Discussion

5.1. Reconstruction of Historical Sediment Storage and Reworking

The model outputs show that D-CASCADE is able to reproduce historical morphological changes in the Bega River network and reconstruct reach (dis)connectivity roles with suitable accuracy. By defining pre-ES boundary conditions and introducing selected drivers of change in the correct temporal sequence, all simulations reproduce both patterns of lowland channel expansion (as seen in Figure 5a) and valley fill incision and material release (Figure 4c; Brooks & Brierley, 1997; Fryirs & Brierley, 2001). By using different discharge scenarios, we can explore and simulate different sediment transport and (dis)connectivity patterns that are driven by different sequences of flood magnitude and frequency.

All simulations also correctly reproduce the role that downstream reaches have played in driving the sediment (dis)connectivity of the basin identified by Fryirs and Brierley (2001). Reaches upstream of the confluence with Wolumla Creek (section A) experience rapid bank erosion and channel expansion after 1850 (Figure 5a). Moderate channel gradient and limited overbank flooding facilitates the transport of newly released sediment down-

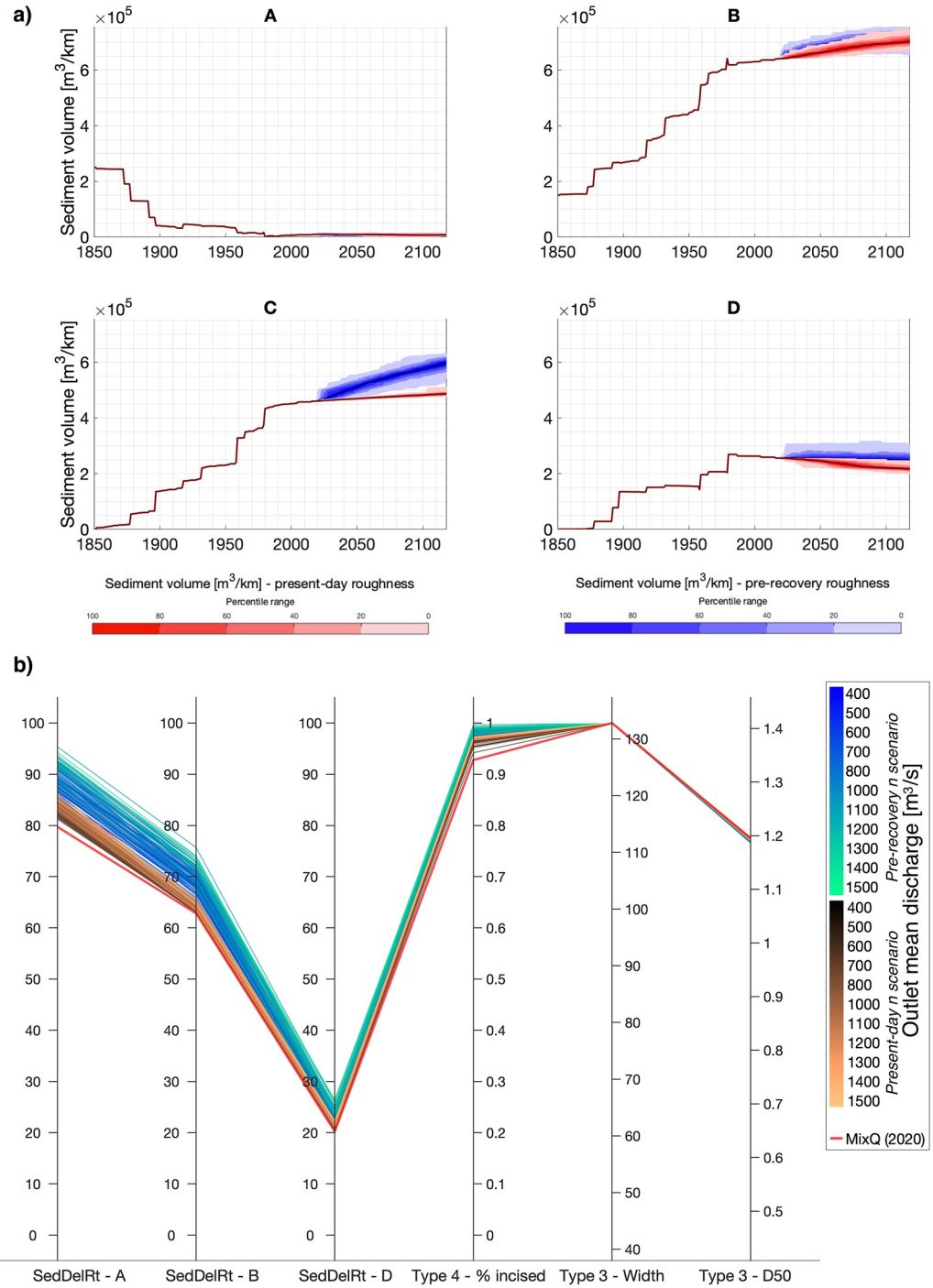

Figure 6. Trajectories and performances of future hydrology scenario, in the pre-restoration and present-day roughness scenarios. (a) Variation of total sediment volume for the downstream sections identified in Figure 4a, from 1850 to 2120, for the two future scenarios. Trajectories from 1850 to 2020 are relative to the MixQ scenario. A Montecarlo fan chart is used to visualize the future trajectories of the parameters after 2020. (b) Performance of the two future hydrology scenario, for the last timestep of the simulation. The red line represents the performance of the MixQ scenario relative to the final year of the historic horizon (2020). The color gradient indicates the mean yearly flood discharge at the outlet for the future trajectories.

stream. After the initialized sediment deposits have been eroded around 1900, these sections switch to transfer zones, where sediment from upstream is quickly conveyed downstream with little or no deposition. The receiving reaches along the lowland plain (sections B-C) behave like sediment sinks, displaying a high degree of sedi-

ment deposition due to low gradients and a high frequency of overbank flooding which limits channel transport capacity. Any sediment that does make it to the gorge in section D is quickly delivered to the basin outlet. This retention effect is greatly exacerbated by the increase in roughness due to vegetative recovery that has occurred since about 1980, as the decrease in transport capacity in the lowland channels leads to less material being mobilized even during large flooding events. Figure 5a shows that the role of the different sections in the sediment connectivity of the basin remains largely the same across the scenarios, with sections A and D as a transfer zone, and B and C as a sediment sinks. This pattern is also confirmed by the sharp decrease in sediment delivery ratio at the lowland plain (Figure 5b, difference between SedDelRatio-A and SedDelRation-D indicators).

For type 4 reaches, all simulations reproduce the high sediment retention rate in valley fill reaches before 1910. However, differences between hydrological scenarios are more evident in the reconstruction of valley fill incision and subsequent sediment release. Only simulations with high discharge for type 4 reaches (HighQ and MixQ) guarantees that most of the material stored in valley fills is mobilized and delivered downstream between 1910 and 2001 (Type 4 - % incised indicator, around 92%, in comparison to the 60% ratio of LowQ). However, sediment release is still noticeably slower when compared to the historic reconstruction. The 1944 aerial photos show that most incision had already occurred, and in the same year MixQ simulation presents a cumulative rate of erosion of 43%. This is probably due to simplifications introduced when modeling sediment entrainment, which is designed to reproduce bank erosion controlled by transport capacity. This approach may not be suitable for simulating complex dynamics of channel incision and gullies formation in eroding valley fills. For future applications, new add-on components for modeling gully formations and channel incision could be implemented to better simulate these processes. Similarly, it is highly likely that the historical adjustments affected channel gradient, thus an add-on designed to model channel slope variations due to sediment accretion and entrainment could be added in future research.

While more exhaustive information on the past hydrology of the basin may have led to better representations of the historical trajectories, the implementation of hydrological scenarios has still yielded satisfactory results, while also providing insight into the sensitivity of geomorphic processes to changes in flood frequency and intensity.

5.2. Future Sediment Release and Transfer

For this system, the model does not suggest that there will be dramatic changes in network-scale sediment (dis) connectivity in coming decades, should the current conditions prevail. The lowland plain will continue to function as a sediment sink, storing the remaining sediment delivered from upstream. By 2120, assuming negligible alterations to present-day riparian vegetation in the lowlands and not accounting for climate change induced hydrological alterations, it is forecast that the increase in sediment delivery ratio will be higher in the reaches located directly downstream of the Wolumla confluence.

These forecast patterns could indicate that while there may be visible variations in sediment delivery along more upstream sections as the tail of the sediment slug reaches the lowland plain, the function of the lowland plain as a sediment sink seems to intensify further downstream. By section C (Figure 6a – red trajectories) this trend is so pronounced that these sections appear mostly insensitive to variation of discharge, significantly stalling the amount of material that can escape to the outlet. The high channel roughness brought by vegetative recovery after 1980 traps virtually all sediment slug material in the lowland plain for the foreseeable future. These results also suggest that should vegetation be removed from the riparian or in-channel zones of the lowland plain, either from wildfires or anthropic interventions, it would trigger a new period of sediment slug mobilization and delivery to the estuary (Figure 6a – blue trajectories).

5.3. Opportunities and Limitations for Further Research

The application of D-CASCADE to the Bega River network showcases the potential of a network-scale dynamic and distributed sediment connectivity model to aid in the reconstruction of historical sediment (dis)connectivity patterns and sediment budget trajectories (Beveridge et al., 2020; Gran & Czuba, 2017; Murphy et al., 2019; Schmitt et al., 2016b). The new dynamic framework allows for the exploration of more complex sediment connectivity processes and how the interactions between different hydro-morphological components that are disaggregated in time and space guide their evolution over time (Czuba, 2018; Wild et al., 2021). This, in turn, makes D-CASCADE a useful instrument for modeling future trends of sediment (dis)connectivity dynamics, and

quantitatively forecasting possible future alterations in time and space resulting from multiple anthropic disturbances in a system.

Furthermore, the flexible and open-ended structure of the D-CASCADE modeling environment allows for the inclusion of multiple add-ons components. The large-scale 1D structure of the model with specific add-ons tools can be used to account for more localized and multidimensional processes in river networks. Dynamic and two-directional interactions between the D-CASCADE model and additional components guarantees that local changes modeled by add-ons can be detected in basin-wide (dis)connectivity analysis (Bracken et al., 2015; Fryirs, 2013). These components may be based on traditional physically based models, or, as in the case of the Bega River case study, simplified relations based on, and calibrated with, historical observations. This provides the advantage of both reducing complexity and uncertainty while producing results that match observed local conditions and known past morphologies. However, the add-ons presented are limited in their applicability, as they are tailored to the specific case study. For example, the channel expansion add-on does not capture the complex morphodynamical processes which drive bank erosion, instead relying on empirical relations based on historical observations to reproduce the channel widening trends. Adaptation and use of these components requires sufficient knowledge of the morphological evolution of the system under investigation.

Compared to traditional morphodynamic modeling, D-CASCADE can successfully simulate sediment transfer at the network scale. Future applications may integrate traditional 3D models with models of local processes, for example, mass failure brought by progressive material removal from the bank toe (see Lammers & Bledsoe, 2018), allowing for more generalized and physics-based modeling albeit with increased data requirements.

D-CASCADE also inherits the limitation of the previous CASCADE framework, as it shares many key modeling concepts (Schmitt et al., 2016b, 2018b). Reach features, hydrology and sediment budget definition via remote sensing data inevitably carries uncertainties. Sediment transport processes are modeled using the same methodologies and class representation everywhere in the network, which may be unrealistic in cases where there is significant heterogeneity in the basin morphology.

The adaptability of D-CASCADE allows hypothesis testing in data-scarce environments where limited data for validation are available. However, modeling complex processes at large spatial and temporal scales does lead to multiple sources of uncertainty, either from the lack of data on boundary conditions, or the modeling parameters necessary to run such large-scale frameworks. Therefore it is important that multiple hypotheses are tested with each simulation (Tangi et al., 2019). Stochastic approaches, like the one used in Schmitt et al. (2018b), and multiple scenario explorations are necessary to test hypotheses on network scale processes and make the results more transparent while "embracing" the uncertainties in modeling sediment (dis)connectivity (Heckmann & Schwanghart, 2013; Shrestha et al., 2021).

Like the original CASCADE model, D-CASCADE is also designed to be employed in strategic decision-making contexts, to provide indicators of sediment (dis)connectivity alteration as part of a multiple decision portfolio (Schmitt et al., 2018a, 2019). The novel dynamic framework allows for the exploration of the competing or compounding effects of time-varying sediment management strategies, for example, basin-wide water release and sediment flushing strategies for multiple reservoirs in different parts of a network (Kondolf, Gao, et al., 2014; Kondolf et al., 2018; Wild et al., 2021). Both uncertainty analysis and portfolio performance exploration are supported by the limited computational requirement and scalability of the D-CASCADE modeling environment, which allows for fast and repeatable model simulation.

The Bega case study offered a unique opportunity to test D-CASCADE, given that so much was already known about the evolution of the rivers and the impact of post-ES disturbance on the morphology of the system over a 170+ year timeframe (Brooks & Brierley, 1997; Brierley & Fryirs, 1998, 1999, 2000; Fryirs & Brierley, 1998, 1999, 2001). This meant that both the boundary conditions and validation parameters could be readily identified and used in the modeling, as well as the transport formulas best suited for this study environment. Despite this, there are still assumptions built into the simulations. Particular work is needed to establish appropriate discharge estimates to run in a place where the length of record is short and patchy. However, the Bega study did allow us to explore the extent to which flows of different magnitude influence different sediment delivery processes and the performance of the model in validation (Frasson et al., 2019). Other complexities include the definition of both sediment transport capacity and sediment velocity and how this can alter spatial and temporal patterns of sediment (dis)connectivity.

Future studies could differentiate between deposition in the channel and on floodplains, by modeling two different sediment layer structures for each reach that store sediment independently, while interacting and exchanging materials to reproduce channel-floodplain interactions (Beveridge et al., 2020; Gilbert & Wilcox, 2020). The representation of sediment deposition shown in Figure 2 assumes no vertical mixing is possible to guarantee proper provenance tracing. Moreover, using the active layer GSD to estimate transport capacity ignores possible discontinuities in the vertical composition of the layer. These hypotheses may not hold for rivers with significant sediment size heterogeneity or frequent bed reworking. Additionally, in rivers characterized by coarser bed grain sizes (gravel or mixed sand and gravel), the effects of vertical bed mixing and material dispersion could render the tracing of individual sediment cascades more challenging to model. Model testing in well monitored case studies may be necessary to validate the framework's effectiveness in these cases.

The simple formulation of sediment velocity, while already used in other distributed sediment models (Czuba, 2018; Czuba et al., 2017; Murphy et al., 2019), has never been exhaustively explored. Given the importance of this parameter for the representation of the movement of sediment volumes, and its inherit complexity and dependence on multiple hydro-morphological features (Ferguson et al., 2015; Gran & Czuba, 2017), further studies on this parameter and how to derive it are necessary. The use of fractional transport capacity equations could allow for the definition of grain size-specific sediment velocities, as in Czuba (2018), which would model sediment delivery via heterogeneous dispersion rather than uniform translation.

Finally, there is work to be done on evaluating the effectiveness of different sediment transport formula at producing sensible and realistic results, particularly if forecasting work is being undertaken and used for river management decision-making.

6. Conclusion

In this study, we present the new dynamic D-CASCADE framework as a promising tool to explore the complex dynamics and patterns of river sediment (dis)connectivity across a catchment and over time. The inclusion of add-ons in the D-CASCADE modeling environment allows for the evaluation of more complex and localized multidimensional morphological processes, which the basic 1D model structure cannot capture.

The D-CASCADE model successfully reproduced the timing and extent of major morphological processes caused by anthropic disturbance of rivers in the Bega River basin, NSW Australia, which included channel expansion, sediment release from upland valley fills and sediment slug formation along the lowland plain. The sediment transport pathways generated by the model generally match the historical reconstruction of sediment supply and delivery ratio. Future trajectories of sediment transport have been conducted to forecast how this system may operate into the future.

The flexible and adaptable potential of the D-CASCADE framework allows for a wide array of future applications, including more complex representations of local morphological processes associated with sediment (dis)connectivity and integration with other large-scale models, for example, distributed hydrological and morphological models and large-scale decision-making frameworks. Limited data requirements and computational time also promote its use for relatively quick testing of model uncertainties and parameter sensitivity for use in final simulations.

Acknowledgments
This research was partially supported by the EC Horizon 2020 Research and Innovation Programme, AMBER Project, grant agreement number 689682. The authors would like to thank all members of the Environmental Intelligence group (www.ei.deib.polimi.it) at Politecnico di Milano who contributed to this work. K. Fryirs acknowledges the financial support of Macquarie University to undertake study leave at the Politecnico of Milano to collaborate on this work, and more recently an ARC Linkage Project (LP190100314) that she leads. Open Access Funding provided by Politecnico di Milano within the CRUI-CARE Agreement.

Data Availability Statement

The data and codes used in this paper are available at https://doi.org/10.5281/zenodo.5841363 and described in Text S3 in Supporting Information S1.

References

Ackers, P., & White, W. R. (1973). Sediment transport: New approach and analysis. *Journal of the Hydraulics Division*, *99*, 2041–2060. https://doi.org/10.1061/JYCEAJ.0003791

Beveridge, C., Istanbulluoglu, E., Bandaragoda, C., & Pfeiffer, A. M. (2020). A channel network model for sediment dynamics over watershed management time scales. *Journal of Advances in Modeling Earth Systems*, *12*, e2019MS001852. https://doi.org/10.1029/2019MS001852

Bizzi, S., Dinh, Q., Bernardi, D., Denaro, S., Schippa, L., & Soncini-Sessa, R. (2015). On the control of riverbed incision induced by run-of-river power plant. *Water Resources Research*, *51*, 5023–5040. https://doi.org/10.1002/2014WR016237

Bizzi, S., Piégay, H., Demarchi, L., Van de Bund, W., Weissteiner, C. J., & Gob, F. (2019). LiDAR-based fluvial remote sensing to assess 50–100-year human-driven channel changes at a regional level: The case of the Piedmont Region, Italy. *Earth Surface Processes and Landforms*, *44*, 471–489. https://doi.org/10.1002/esp.4509

Bizzi, S., Tangi, M., Schmitt, R. J., Pitlick, J., Piégay, H., Castelletti, A. F. (2021). Sediment transport at the network scale and its link to channel morphology in the braided Vjosa River system. *Earth Surface Processes and Landforms*, *46*(14), 2946–2962. http://doi.org/10.1002/esp.5225

Bracken, L. J., Turnbull, L., Wainwright, J., & Bogaart, P. (2015). Sediment connectivity: A framework for understanding sediment transfer at multiple scales. *Earth Surface Processes and Landforms*, *40*, 177–188. https://doi.org/10.1002/esp.3635

Briere, C., Giardino, A., & van der Werf, J. (2010). *Morphological modeling of bar dynamics with Delft3d: The quest for optimal free parameter settings using an automatic calibration technique*. https://doi.org/10.9753/icce.v32.sediment.60

Brierley, G. J., Cohen, T., Fryirs, K., & Brooks, A. (1999). Post-European changes to the fluvial geomorphology of Bega catchment, Australia: Implications for river ecology. *Freshwater Biology*, *41*, 839–848. https://doi.org/10.1046/j.1365-2427.1999.00397.x

Brierley, G. J., & Fryirs, K. (1998). A fluvial sediment budget for upper Wolumla Creek, south coast, New South Wales, Australia. *Australian Geographer*, *29*, 107–124. https://doi.org/10.1080/00049189808703206

Brierley, G. J., & Fryirs, K. (1999). Tributary–trunk stream relations in a cut-and-fill landscape: A case study from Wolumla catchment, New South Wales, Australia. *Geomorphology*, *28*, 61–73. https://doi.org/10.1016/s0169-555x(98)00103-2

Brierley, G. J., & Fryirs, K. (2000). River styles, a geomorphic approach to catchment characterization: Implications for river rehabilitation in Bega catchment, New South Wales, Australia. *Environmental Management*, *25*, 661–679. https://doi.org/10.1007/s002670010052

Brierley, G. J., & Fryirs, K. A. (2013). *Geomorphology and river management: Applications of the river styles framework*. John Wiley & Sons.

Brooks, A. P., & Brierley, G. J. (1997). Geomorphic responses of lower Bega River to catchment disturbance, 1851–1926. *Geomorphology*, *18*, 291–304. https://doi.org/10.1016/S0169-555X(96)00033-5

Cardno (2018). *Floodplain Risk Management Study - Bega River. Bega Valley Shire Council 214*. Retrieved from https://begavalley.nsw.gov.au/cp_content/resources/bega_brogo_rivers_final_FRMS(1).pdf

Czuba, J. A. (2018). A Lagrangian framework for exploring complexities of mixed-size sediment transport in gravel-bedded river networks. *Geomorphology*, *321*, 146–152. https://doi.org/10.1016/j.geomorph.2018.08.031

Czuba, J. A., & Foufoula-Georgiou, E. (2014). A network-based framework for identifying potential synchronizations and amplifications of sediment delivery in river basins. *Water Resources Research*, *50*, 3826–3851. https://doi.org/10.1002/2013WR014227

Czuba, J. A., Foufoula-Georgiou, E., Gran, K. B., Belmont, P., & Wilcock, P. R. (2017). Interplay between spatially explicit sediment sourcing, hierarchical river-network structure, and in-channel bed material sediment transport and storage dynamics. *Journal of Geophysical Research: Earth Surface*, *122*, 1090–1120. https://doi.org/10.1002/2016JF003965

Demarchi, L., Bizzi, S., & Piégay, H. (2017). Regional hydromorphological characterization with continuous and automated remote sensing analysis based on VHR imagery and low-resolution LiDAR data. *Earth Surface Processes and Landforms*, *42*, 531–551. https://doi.org/10.1002/esp.4092

Ferguson, R. I., Church, M., Rennie, C. D., & Venditti, J. G. (2015). Reconstructing a sediment pulse: Modeling the effect of placer mining on Fraser River, Canada. *Journal of Geophysical Research: Earth Surface*, *120*, 1436–1454. https://doi.org/10.1002/2015JF003491

Frasson, R. P. D. M., Pavelsky, T. M., Fonstad, M. A., Durand, M. T., Allen, G. H., Schumann, G., et al. (2019). Global relationships between river width, slope, catchment area, meander wavelength, sinuosity, and discharge. *Geophysical Research Letters*, *46*, 3252–3262. https://doi.org/10.1029/2019GL082027

Fryirs, K. (2013). (Dis)Connectivity in catchment sediment cascades: A fresh look at the sediment delivery problem. *Earth Surface Processes and Landforms*, *38*, 30–46. https://doi.org/10.1002/esp.3242

Fryirs, K., & Brierley, G. (2005). *Practical applications of the river styles framework as a tool for catchment-wide river management: A case study from Bega catchment*. (p. 227) Macquirie University. https://riverstyles.com/wp-content/uploads/2019/05/Bega-ch-1.pdf

Fryirs, K., & Brierley, G. J. (1998). The character and age structure of valley fills in upper Wolumla Creek catchment, south coast, New South Wales, Australia. *Earth Surface Processes and Landforms* (Vol. *23*, pp. 2712–2875). https://doi.org/10.1002/(sici)1096-9837(199803)23:3<271::aid-esp867>3.0.co;2-5

Fryirs, K., & Brierley, G. J. (1999). Slope–channel decoupling in Wolumla catchment, New South Wales, Australia: The changing nature of sediment sources following European settlement. *CATENA*, *35*, 41–63. https://doi.org/10.1016/S0341-8162(98)00119-2

Fryirs, K., & Brierley, G. J. (2001). Variability in sediment delivery and storage along river courses in Bega catchment, NSW, Australia: Implications for geomorphic river recovery. *Geomorphology*, *38*, 237–265. https://doi.org/10.1016/S0169-555X(00)00093-3

Fryirs, K. A., Brierley, G. J., Hancock, F., Cohen, T. J., Brooks, A. P., Reinfelds, I., et al. (2018). Tracking geomorphic recovery in process-based river management. *Land Degradation & Development*, *29*, 3221–3244. https://doi.org/10.1002/ldr.2984

Fryirs, K. A., Brierley, G. J., Preston, N. J., & Kasai, M. (2007). Buffers, barriers and blankets: The (dis) connectivity of catchment-scale sediment cascades. *Catena*, *70*, 49–67. https://doi.org/10.1016/j.catena.2006.07.007

Gilbert, J. T., & Wilcox, A. C. (2020). Sediment routing and floodplain exchange (SeRFE): A spatially explicit model of sediment balance and connectivity through river networks. *Journal of Advances in Modeling Earth Systems*, *12*, e2020MS002048. https://doi.org/10.1029/2020MS002048

Gran, K. B., & Czuba, J. A. (2017). Sediment pulse evolution and the role of network structure. *Geomorphology, Connectivity in Geomorphology from Binghamton*, *277*, 17–30. https://doi.org/10.1016/j.geomorph.2015.12.015

Gregory, K. J. (2019). Human influence on the morphological adjustment of river channels: The evolution of pertinent concepts in river science. *River Research and Applications*, *35*, 1097–1106. https://doi.org/10.1002/rra.3455

Hassan, M. A., Church, M., & Schick, A. P. (1991). Distance of movement of coarse particles in gravel bed streams. *Water Resources Research*, *27*, 503–511. https://doi.org/10.1029/90WR02762

Heckmann, T., Cavalli, M., Cerdan, O., Foerster, S., Javaux, M., Lode, E., et al. (2018). Indices of sediment connectivity: Opportunities, challenges and limitations. *Earth-Science Reviews*, *187*, 77–108. https://doi.org/10.1016/j.earscirev.2018.08.004

Heckmann, T., & Schwanghart, W. (2013). Geomorphic coupling and sediment connectivity in an alpine catchment — Exploring sediment cascades using graph theory. *Geomorphology*, *182*, 89–103. https://doi.org/10.1016/j.geomorph.2012.10.033

Kondolf, G. M., Gao, Y., Annandale, G. W., Morris, G. L., Jiang, E., Zhang, J., et al. (2014). Sustainable sediment management in reservoirs and regulated rivers: Experiences from five continents. *Earth's Future*, *2*, 256–280. https://doi.org/10.1002/2013EF000184

Kondolf, G. M., Rubin, Z. K., & Minear, J. T. (2014). Dams on the Mekong: Cumulative sediment starvation. *Water Resources Research*, *50*, 5158–5169. https://doi.org/10.1002/2013WR014651

Kondolf, G. M., Schmitt, R. J. P., Carling, P., Darby, S., Arias, M., Bizzi, S., et al. (2018). Changing sediment budget of the Mekong: Cumulative threats and management strategies for a large river basin. *Science of the Total Environment*, *625*, 114–134. https://doi.org/10.1016/j.scitotenv.2017.11.361

Lammers, R. W., & Bledsoe, B. P. (2018). A network scale, intermediate complexity model for simulating channel evolution over years to decades. *Journal of Hydrology*, *566*, 886–900. https://doi.org/10.1016/j.jhydrol.2018.09.036

Manning, R., Griffith, J. P., Pigot, T. F., & Vernon-Harcourt, L. F. (1890). *On the flow of water in open channels and pipes*.

Merritt, W. S., Letcher, R. A., & Jakeman, A. J. (2003). A review of erosion and sediment transport models. *Environmental Modelling & Software*, The Modelling of Hydrologic Systems, *18*, 761–799. https://doi.org/10.1016/S1364-8152(03)00078-1

Molinas, A., & Wu, B. (2000). Comparison of fractional bed-material load computation methods in sand-bed channels. *Earth Surface Processes and Landforms*, *25*, 1045–1068. https://doi.org/10.1002/1096-9837(200009)25:10<1045::AID-ESP115>3.0.CO;2-X

Murphy, B. P., Czuba, J. A., & Belmont, P. (2019). Post-wildfire sediment cascades: A modeling framework linking debris flow generation and network-scale sediment routing. *Earth Surface Processes and Landforms*, *44*, 2126–2140. https://doi.org/10.1002/esp.4635

Pilgrim, E., Pilgrim, D., & Canterford, R. (1987). *Australian rainfall and runoff: A guide to flood estimation*. Institution of Engineers.

Poeppl, R. E., Fryirs, K. A., Tunnicliffe, J., & Brierley, G. J. (2020). Managing sediment (dis)connectivity in fluvial systems. *Science of the Total Environment*, *736*, 139627. https://doi.org/10.1016/j.scitotenv.2020.139627

Schmitt, R. J. P., Bizzi, S., & Castelletti, A. (2016). Tracking multiple sediment cascades at the river network scale identifies controls and emerging patterns of sediment connectivity. *Water Resources Research*, *52*, 3941–3965. https://doi.org/10.1002/2015WR018097

Schmitt, R. J. P., Bizzi, S., Castelletti, A., & Kondolf, G. M. (2018). Improved trade-offs of hydropower and sand connectivity by strategic dam planning in the Mekong. *Nature Sustainability*, *1*, 96–104. https://doi.org/10.1038/s41893-018-0022-3

Schmitt, R. J. P., Bizzi, S., Castelletti, A., Opperman, J. J., & Kondolf, G. M. (2019). Planning dam portfolios for low sediment trapping shows limits for sustainable hydropower in the Mekong. *Science Advances*, *5*, eaaw2175. https://doi.org/10.1126/sciadv.aaw2175

Schmitt, R. J. P., Bizzi, S., & Castelletti, A. F. (2014). Characterizing fluvial systems at basin scale by fuzzy signatures of hydromorphological drivers in data scarce environments. *Geomorphology*, *214*, 69–83. https://doi.org/10.1016/j.geomorph.2014.02.024

Schmitt, R. J. P., Bizzi, S., & Castelletti, A. F. (2016). Tracking multiple sediment cascades at the river network scale identifies controls and emerging patterns of sediment connectivity. *Water Resources Research*, *52*, 3941–3965. https://doi.org/10.1002/2015WR018097

Schmitt, R. J. P., Bizzi, S., Castelletti, A. F., & Kondolf, G. M. (2018). Stochastic Modeling of Sediment Connectivity for Reconstructing Sand Fluxes and Origins in the Unmonitored Se Kong, Se San, and Sre Pok Tributaries of the Mekong River: Stochastic connectivity modelling. *Journal of Geophysical Research: Earth Surface*, *123*, 2–25. https://doi.org/10.1002/2016JF004105

Schwanghart, W., & Scherler, D. (2014). Short communication: TopoToolbox 2 – MATLAB-based software for topographic analysis and modeling in Earth surface sciences. *Earth Surface Dynamics*, *2*, 1–7. https://doi.org/10.5194/esurf-2-1-2014

Shrestha, B., Cochrane, T. A., Caruso, B. S., Arias, M. E., & Wild, T. B. (2021). Sediment management for reservoir sustainability and cost implications under land use/land cover change uncertainty. *Water Resources Research*, *57*, e2020WR028351. https://doi.org/10.1029/2020WR028351

Sklar, L. S., Riebe, C. S., Marshall, J. A., Genetti, J., Leclere, S., Lukens, C. L., & Merces, V. (2017). The problem of predicting the size distribution of sediment supplied by hillslopes to rivers. *Geomorphology, Connectivity in Geomorphology from Binghamton*, *277*, 31–49. https://doi.org/10.1016/j.geomorph.2016.05.005

Stevens, H. H., Jr, & Yang, C. T. (1989). Summary and use of selected fluvial sediment-discharge formulas (No. 89–4026). In *Water-Resources Investigations Report*. U.S. Geological Survey : Open-File Services SectionWestern Distribution Branch. https://doi.org/10.3133/wri894026

Surian, N., & Rinaldi, M. (2003). Morphological response to river engineering and management in alluvial channels in Italy. *Geomorphology*, *50*, 307–326. https://doi.org/10.1016/S0169-555X(02)00219-2

Tangi, M., Schmitt, R., Bizzi, S., & Castelletti, A. (2019). The CASCADE toolbox for analyzing river sediment connectivity and management. *Environmental Modelling & Software*, *119*, 400–406. https://doi.org/10.1016/j.envsoft.2019.07.008

Vörösmarty, C. J., Meybeck, M., Fekete, B., Sharma, K., Green, P., & Syvitski, J. P. M. (2003). Anthropogenic sediment retention: Major global impact from registered river impoundments. *Global and Planetary Change, The supply of flux of sediment along hydrological pathways: Anthropogenic influences at the global scale*, *39*, 169–190. https://doi.org/10.1016/S0921-8181(03)00023-7

Wasson, R. J. (1994). Annual and decadal variation of sediment yield in Australia, and some global comparisons. *IAHS Publications-Series of Proceedings and Reports-Intern Assoc Hydrological Sciences*, *11*.

Wasson, R. J., Olive, J. R., & Rosewell, C. J. (1996). Rates of erosion and sediment transport in Australia. In *Erosion and sediment yield: Global and regional perspectives: Proceedings of an international symposium held at Exeter, UK* (Vol. 11).

Wild, T. B., Birnbaum, A. N., Reed, P. M., & Loucks, D. P. (2021). An open source reservoir and sediment simulation framework for identifying and evaluating siting, design, and operation alternatives. *Environmental Modelling & Software*, *136*, 104947. https://doi.org/10.1016/j.envsoft.2020.104947

Wohl, E., Brierley, G. J., Cadol, D., Coulthard, T. J., Covino, T., Fryirs, K. A., et al. (2019). Connectivity as an emergent property of geomorphic systems. *Earth Surface Processes and Landforms*, *44*, 4–26. https://doi.org/10.1002/esp.4434

Wu, W., & Wang, S. S. Y. (2006). Formulas for sediment porosity and settling velocity. *Journal of Hydraulic Engineering*, *132*, 858–862. https://doi.org/10.1061/(asce)0733-9429(2006)132:8(858)

Yamazaki, D., O'Loughlin, F., Trigg, M. A., Miller, Z. F., Pavelsky, T. M., & Bates, P. D. (2014). Development of the global width database for large rivers. *Water Resources Research*, *50*, 3467–3480. https://doi.org/10.1002/2013WR014664